Northern hemispheric atmospheric ethane trends in the upper troposphere and lower stratosphere (2006-2016) with reference to methane and propane

5   Mengze Li [1,2], Andrea Pozzer [1], Jos Lelieveld [1,3], Jonathan Williams [1,3]

1 Max Planck Institute for Chemistry, Hahn-Meitner-Weg 1, 55128 Mainz, Germany

2 Now at: Department of Climate and Space Sciences and Engineering, University of Michigan, Ann Arbor, USA

3 Climate and Atmosphere Research Center, The Cyprus Institute, 1645, Nicosia, Cyprus

Correspondence to: Jonathan Williams (jonathan.williams@mpic.de); Mengze Li (mengzel@umich.edu)

10

Abstract. Methane, ethane, and propane are among the most abundant hydrocarbons in the atmosphere. These compounds have many emission sources in common and are all primarily removed through OH oxidation. Their mixing ratios and long-term trends in the upper troposphere and stratosphere are rarely reported due to the paucity of measurements. In this study, we present long-term (2006-2016) northern hemispheric ethane, propane, and methane
15 data from airborne observation in the Upper Troposphere - Lower Stratosphere (UTLS) region from IAGOS-CARIBIC project. The methane and propane observations provide additional information for understanding northern hemispheric ethane trends, which is the major focus of this study. The linear trends, moving averages, non-linear trends and monthly variations of ethane, methane and propane in 2006-2016 were presented for the upper troposphere and lower stratosphere over five regions (whole Northern Hemisphere, Europe, North America, Asia and
20 rest of the world). The growth rates of ethane, methane, and propane in the upper troposphere are -2.24, 0.33, and -0.78 %/yr, respectively, and in the lower stratosphere they are -3.27, 0.26, and -4.91 %/yr, respectively, in 2006-2016. This dataset is of value to future global ethane budget estimates and the optimization of current ethane inventories. The data are publicly accessible at https://doi.org/10.5281/zenodo.6536109 (Li et al., 2022).

1. Introduction

Ethane (C_2H_6) is among the most abundant non-methane hydrocarbons (NMHC) present in the atmosphere. Major sources of ethane to the atmosphere are via natural gas and oil production (~62%), biofuel combustion (20%), and biomass burning (18%). Interestingly, 84% of its total emissions are from the Northern Hemisphere (NH) (Xiao et al., 2008). Oxidation by hydroxyl (OH) radicals is the major atmospheric loss process for tropospheric ethane, while in the stratosphere the reaction with chlorine (Cl) radicals provides an additional loss process (Li et al., 2018). Due to the seasonal variation of ethane emissions and the photochemically generated OH radicals, ethane has a clear annual cycle in mole fractions, showing higher levels in winter. Its global lifetime is circa three months, with a minimum in summer (~2 months) and a maximum in winter (~10 months) (Xiao et al., 2008; Helmig et al., 2016; Li et al., 2018). Ethane oxidation forms acetaldehyde, which in turn contributes to the formation of PAN (peroxyacetyl nitrate) or peracetic acid depending on the levels of NO_x (Millet et al., 2010). PAN acts as a reservoir species of nitrogen oxides (NO_x) and can strongly affect tropospheric ozone distributions by transporting NO_x from the point of emission to remote locations. Furthermore, PAN is known to be a secondary pollutant like ozone with negative impacts on regional air quality and human health (Rudolph, 1995; González Abad et al., 2011; Fischer et al., 2014; Monks et al., 2018; Kort et al., 2016; Tzompa-Sosa et al., 2017; Dalsøren et al., 2018; Pozzer et al., 2020).

Many studies have reported ethane trend analysis based on either ground-based sampling or FTIR (Fourier Transform Infrared Spectrometer) measurements. A summary of these studies is shown in Table 1. In the troposphere (Table 1a), a decreasing trend of ethane during 1986-2008 and an increasing trend during 2009-2014 were reported in the literature. The trends of C_2H_6 partial column at four European sites (Jungfraujoch, Zugspitze, Harestua and Kiruna) during 1996-2006 were between about -1.09 to -2.11%/yr (Angelbratt et al., 2011). Simpson et al. (2012) concluded a strong global ethane decline of 21% over 26 years (1984-2010), with a stronger decline occurring from 1984 to 1999 (-7.2 ± 1.7 ppt/yr) than from 2000 to 2010 (-1.9 ± 1.3 ppt/yr). Franco et al. (2015) showed the ethane trend at Jungfraujoch to be -0.92%/yr during 1994-2008, followed by a strong positive trend of 4.9%/yr during 2009-2014, which may be related to the intensifying emissions from shale gas exploitation in North America. Helmig et al. (2016) calculated a mean ethane growth rate of 2.9-4.7%/yr from 2009 to 2014 at 32 NH ground measurement sites and

concluded that North American oil and gas development was the primary source of the increasing

55　emission of ethane. Franco et al. (2016) compared the ethane total column change at six sites across NH for the period of 2003-2008 and 2009-2014, and also revealed a sharp increase of 3-5%/yr during 2009-2014 compared with 2003-2008, which was associated with oil and gas industry emission. Hausmann et al. (2016) presented a positive ethane trend of ca. 4.6%/yr at Zugspitze (47° N) and a negative trend of ca. -2.5%/yr at Lauder (45° S) for 2007-2014, and inferred an ethane

60　increase from oil and gas emission of 1-11 Tg/yr for 2007-2014. Angot et al. (2021) showed an increasing trend in ethane of ca. 5.6%/yr at GEOSummit (73°N) for 2010-2014, followed by a temporary pause of ethane growth in 2015-2018. Sun et al. (2021) presented a negative ethane trend of -2.6 ± 1.3%/yr over 2015-2020 in a densely populated eastern Chinese city Hefei.

In contrast to tropospheric ethane trends, trends in the stratosphere have been far less investigated.

65　The stratospheric ethane trends were reported to follow a decreasing trend in 1995-2008 and an increasing trend in 2009-2015 (Table 1b). Gardiner et al. (2008) presented the annual trend in stratospheric ethane column (relative to year 2000) at six sites and these varied from 0.43 to -3.31%/yr until the year 2005. Franco et al. (2015) reported ethane trends at 8-16 km measured at Jungfraujoch of -1.75 ± 1.30%/yr for 2004-2008 and 9.4 ± 3.2%/yr for 2009-2013, indicating an

70　~11% sharp increase since 2009. Helmig et al. (2016) showed that the UTLS column ethane (8-21km) measured at Jungfraujoch was decreasing by -1.0 ± 0.2%/yr from 1995 to 2009, and started a sharp increase at a rate of 6.0 ± 1.1%/yr from 2009 until 2015, while the difference in growth rate between the two time periods is smaller for the mid-tropospheric column (3.6-8 km): -0.8 ± 0.3%/yr (1995-2009) and 4.2 ± 1.0%/yr (2009-2015).

75　Previous investigations of the distribution, emissions, lifetime, and atmospheric trends of ethane have been mostly based on surface-based measurements. These have been either from a regionally focused intensive field measurement campaign (e.g. Kort et al. (2016)) or from networks of remote sampling stations (e.g. Franco et al. (2015), Helmig et al. (2016)). The advantage of surface sites is that they are easily accessed and maintained, however, such

80　measurements inevitably reflect the local or regional situation, and changes in emissions immediately upwind of a measurement location can affect the results, masking any underlying long-term global trend. In addition, most ethane measurement sites are located in high-income countries, such as North America and Europe, while ethane observations in the rest of the world

are sparse. This too hinders the assessment of global ethane trends, for while one country's

85 emission may be declining another's could be increasing rapidly. For the aforementioned reasons, it is advantageous to assess the global long-term ethane trend from the upper troposphere and even the stratosphere where emissions can be expected to be well mixed by atmospheric circulations. In particular, the trend of ethane in the more isolated and remote stratosphere is of interest when assessing long-term changes.

90 In this study, we use airborne observations covering the Northern Hemisphere (NH), including regions without ground measurements. We present long-term northern hemispheric and geographically delineated (North America, Asia, Europe, Rest of the world) ethane trends in the upper troposphere and lower stratosphere for the decade 2006-2016 derived using airborne measurements. In addition, the trends of methane and propane collected from the same

95 observations are examined to better understand the observed variation of NH ethane trends, as they have common sources and sinks in the atmosphere. This study focuses on describing the dataset itself, therefore, an in depth interpretation is outside the scope. All the data used in this study are publicly available at https://doi.org/10.5281/zenodo.6536109. These data can be used for further analysis on global and regional trends, emissions and lifetime of methane, ethane, and propane,

100 their contributions to climate change, troposphere-stratosphere exchange, and improvement of current inventories and atmospheric models.

2. Materials and Methods

2.1 IAGOS-CARIBC observation

105 The IAGOS-CARIBIC project (In-service Aircraft for a Global Observing System-Civil Aircraft for the Regular Investigation of the atmosphere Based on an Instrument Container) is an aircraft-based scientific project with the aim of monitoring long-term global atmospheric physics and chemistry (Brenninkmeijer et al., 2007). The flight altitudes are at ~10 km, which is in the Upper Troposphere-Lower Stratosphere (UTLS) region. A custom-built whole air sampler collects

110 pressurized air samples during each flight, and these samples are subsequently measured in the laboratory with Gas Chromatography (GC) coupled with three detectors: GC-ECD (for carbon

dioxide, nitrous oxide, and sulphur hexafluoride) (Schuck et al., 2009), GC-FID for methane and volatile organic compounds (including ethane and propane)(Baker et al., 2010), and GC-AED for volatile organic compound measurements after 2017 (data not used in this study) (Karu et al., 2021) (Karu et al., 2021). The precision of ethane and propane data used in this study is 0.2% and 0.8%, respectively (Baker et al., 2010), and of methane 0.17% (Schuck et al., 2009). Details regarding operational and analytical procedures, calibration scales, and quality assurance are documented in the cited references, and summarized as follows.

Each IAGOS-CARIBIC flight normally consists of four flight sequences with a total number of 116 air samples collected by whole air samplers (flasks). The inlet and outlet of each flask are connected by multi-position valves which can be automatically switched with programming. A pumping system and pressure sensors are connected to the inlet valves to guarantee the final pressure in each flask to be around 4.5 bar. The outlet valves are connected to ambient air. Prior to pressurization, each flask is flushed with ambient air for 10 times (about 5-10 min). The average filling (sampling) time of each flask is about 45s (range 0.5-1.5 min) depending on the flight altitude, resulting a spatial resolution of 7-21km.

Methane (CH_4), ethane (C_2H_6), and propane (C_3H_8) were measured with a HP 6890 GC with a polymer Porapak Q 3/4" column (10 ft, 100/120 mesh) installed in a single oven. Nitrogen (N_2, purity 99.999%) was used as carrier gas at a constant flow rate of 50ml/min. The GC was operated at oven temperature of 220°C with flow rates of synthetic air of 250ml/min and hydrogen of 80ml/min. Water vapor in samples was removed by passing through a drying tube at the start of the analysis. The calibration standards and reference gas cylinders were ordered from NOAA (for methane), and the National Physical Laboratory (for ethane and propane) which are certified against World Meteorological Organization (WMO) Global Atmosphere Watch (GAW) program scale, and they are regularly renewed within every three years which warrants the stability of calibration gases. Three additional calibration standards samples were measured in between samples of each flight sequence in order to monitor the quality of measurements and reduce uncertainty.

In total 6,607 Northern Hemispheric samples were collected during Feb 2006-Feb 2016. The overview of geographical distribution, altitude, PV, ethane, methane and propane of all 6,607 samples collected in 2006-2016 is shown in Figure 1. Samples were collected in a broad range of

latitude (0.2 – 77.4°) and longitude (-122.2 – 141.8°) (Figure 1a). 57.9% of the samples were collected in the latitude bands of 30-60°, 25.6% were from latitude 0-30°, and 16.5% from latitude above 60°. Samples were collected at altitude range of 946.4 – 12,525.1 m, with 98.8% being collected above 8,000 m (Figure 1b). PV values of all the samples range from -0.32 – 12.17 (Figure 1c). For the trend analyses in the later sections, samples collected at altitude lower than 8,000 m and PV<2 PVU were excluded. 74 samples were collected at altitude lower than 8,000 m and Potential Vorticity (PV) <2 PVU (Potential Vorticity Unit), where can be largely influenced by surface emissions. Therefore, those samples were excluded from trend analyses. The remaining 6,533 samples were divided into two categories: upper tropospheric samples (altitude ≥ 8,000 m and PV < 2 PVU), and lower stratospheric samples (PV ≥ 2 PVU). To investigate the changes above the tropopause, the lower stratospheric samples were classified into the lower part of the lower stratosphere (2 PVU ≤ PV < 6 PVU) and the upper part (PV ≥ 6 PVU). All samples are categorized into four regions based on their sampling locations: North America (NAM), Asia (ASI), Europe (EUR), and Rest of Northern Hemisphere (RNH). The coordinate of each region is shown in Table S1 and geographical distribution of samples is shown in Figure S1 in the Supplementary Material. In later analyses, we used the term "whole NH" to refer to the combination of four regions. Table 2 shows the total sample number collected in 2006-2016 of 20 sub-regions, i.e. 4 categories (upper troposphere, lower stratosphere, lower stratosphere-lower part, lower stratosphere-upper part) and 5 regions (whole NH, EUR, NAM, ASI, RNH). The later sections will further investigate the trends and seasonality of ethane, methane and propane in these 20 sub-regions. It is noted that the region designated does not correspond to the source region, only the geographical location of the data points.

2.2 Trend analysis

We have applied three trend analysis methods in this study: linear fit, moving average, and non-linear trend.

(1) Linear fit was applied to each sub-region throughout the entire time period (2006-2016). The growth rates of ethane, methane and propane of each sub-region by linear fit are shown in Table 2. These growth rates were referred as "linear trend" in the later sections.

(2) Moving average was achieved with Python (version 3.9.7) pandas package DataFrame.rolling function using a rolling sum with a window length of 20 observations.

(3) Non-linear trend analysis using the "Prophet" algorithm (Taylor and Letham, 2018). The "Prophet" algorithm has been applied on the analysis of non-continuous time-series datasets (Li et al., 2022), as is the case for aircraft data. The trend analysis model has four components: trend (non-periodic changes), seasonality (periodic changes), holiday effects, and error (idiosyncratic changes). In this study, effects of holidays are not included. We used a linear model with change points for the trend component, and the trend function consists of growth rate, adjustments of growth rate, and offset parameter. The flexibility of trend (e.g. overfitting or underfitting) can be adjusted by the parameter "changepoint_prior_scale". A change point represents the moments where the data shifts directions. The value of the parameter "changepoint_prior_scale" represents the strength of change points, more change points will be automatically detected when the value of this parameter increases. The uncertainty interval was set to be 95%. The code of trend analysis in Python for this study can be found in the Supplementary Material. Figure S2 shows the ethane trend and seasonality at Iceland estimated by "Prophet" algorithm. Compared with the trend and seasonality estimated by the NOAA algorithm (www.esrl.noaa.gov/gmd/ccgg/mbl/crvfit/crvfit.html) using the same dataset in Figure 1(b) of Helmig et al. (2016), the seasonality of ethane is captured by both algorithms and the results match with each other. The non-linear trend is estimated as the average value of ten fitting levels on the trend (i.e. "changepoint_prior_scale" = 0.1, 0.2, 0.3, …, 0.9, 1.0).

The uncertainty of the non-linear trend analysis is estimated by resampling methods. For the dataset of each sub-region, we randomly resampled the dataset 20 times, with each time consisting 90% of the samples of the dataset. We then run the "Prophet" algorithm for each of the 20 sub datasets, using the average value of ten fitting levels as the trend of each sub dataset. The range of the 20 trends from the resampled datasets is assumed as the uncertainty of non-linear trend analysis for each sub-region.

3. Results and Discussion

3.1 Overview of IAGOS-CARIBC observations

Figures 1 d,e,f show the observed ethane, methane and propane mole fractions, their linear trends over 2006-2016, and their moving average. The observed mole fractions of ethane, methane and propane are in the range of 5.5 – 2982.2 ppt, 1579.7 – 1926.8 ppb, and 1.0 – 2090.0 ppt, respectively.

205   Both ethane and propane showed decreasing trends using linear fit over 2006-2016, and methane had an increasing growth rate over the same period. The exact growth rates of ethane, methane, and propane are not reported here, however, they are reported in the later sections where regional trends are investigated.

210   ## 3.2 Upper tropospheric trends

3.2.1 Linear trends in the upper troposphere

Figure 2 shows the upper tropospheric observations, linear trends and moving average of ethane (Figures 2 a,b,c,d,e), methane (Figures 2 f,g,h,i,j) and propane (Figures 2 k,l,m,n,o) over five regions: whole Northern Hemisphere (Figures 2 a,f,k), Europe (Figures 2 b,g,l), North America

215   (Figures 2 c,h,m), Asia (Figures 2 d,i,n), and rest of the world (Figures 2 e,j,o). The growth rates of ethane, methane and propane over each region are shown in Table 2 a.

The upper tropospheric ethane shows decreasing trends over all regions for 2006-2016, with the most decrease in RNH (-26.7 ppt/yr, -5.19 %/yr) and the least decrease in ASI (-6.9 ppt/yr, -1.17 %/yr). The whole NH upper tropospheric ethane decreased at a rate of -14.9 ppt/yr (-

220   2.24 %/yr) over 2006-2016. Unlike the large variations in linear trends of ethane among regions, the upper tropospheric methane shows more homogeneous increasing trends among all regions (range 5.2-6.7 ppb/yr, 0.29-0.37 %/yr) due to its longer atmospheric lifetime. The whole NH upper tropospheric propane decreased at rate of -0.7 ppt/yr (-0.78 %/yr), which is dominated by the decrease in RNH (-7.5 ppt/yr, 14.7 %/yr). The upper tropospheric propane mole fractions

225   were increasing at rates of 0.3 – 3.2 ppt/yr (0.33 – 2.1 %/yr) in EUR, ASI and NAM.

3.2.2 Non-linear trends in the upper troposphere

The non-linear trends of upper tropospheric ethane, methane, and propane at regional scales, estimated by the "Prophet" algorithm and their associated uncertainties are shown in Figure 3.

230 Ethane and methane share common sources in gas and oil emissions, and ethane, methane, and propane react with OH radicals as their major sinks in the troposphere.

In early 2010, a peak is clear to be seen for all three compounds in the whole NH upper troposphere, which may indicate a decrease in OH radicals. This peak is also pronounced in ASI for all three compounds, however, the methane peak in ASI has large uncertainty.

235 Ethane and propane in EUR are noticeably higher than other regions due to lower sampling altitudes in EUR (Figure S3, mean ± one standard deviation, 10,197 ± 857 m) compared to other regions (NAM: 10,982 ± 557 m; ASI: 10,621 ± 942 m; RNH: 11,054 ± 580 m). Whereas methane in EUR is at similar level to other regions due to methane's longer atmospheric lifetime.

Large uncertainties occur when the sampling number was low (<100). For example, the trend
240 uncertainties for ethane, methane and propane in ASI were large during Jan 2009-Nov 2011, because most ASI samples were collected during Jun-Oct 2010, and there was a 1.5 year gap between Jan 2009 and Jun 2010 when no sample was collected (Figure 2).

3.2.3 Monthly variation in the upper troposphere

245 The monthly variations of the observed upper tropospheric ethane, methane and propane mole fractions (2006-2016) over five regions (whole NH, EUR, NAM, ASI and RNH) are shown in Figure 4. The observed monthly variations are driven by the emissions and atmospheric hydroxyl radical (OH) cycle (the major sink for tropospheric ethane, methane and propane). The whole NH upper tropospheric ethane, methane and propane mole fractions show peaks in June and July. The
250 upper tropospheric NAM and EUR ethane mole fractions increase from October/November peaking in April, decrease from April until October. This is consistent with the FTIR observation (Franco et al., 2015). The upper tropospheric ASI and RNH ethane peaks in June, two months later than NAM and EUR. Methane shows small monthly variations in EUR, NAM and RNH, suggesting that the emissions play a greater role and thus compensate the influence of the
255 seasonal cycle of OH radical. The upper tropospheric methane in ASI has shown higher mole fractions in summer (June-September) due to deep convection of upward transport of surface air

with higher methane into the upper troposphere during Asian monsoon (Baker et al., 2012). The monthly variations of propane are more variable compare to ethane due to the shorter lifetime of propane and probably more variable emission sources of propane.

260

3.3 Lower stratospheric trends

The sources and sinks of ethane, methane and propane in the stratosphere are different as in the troposphere. There is no known large emission source of ethane, methane and propane in the stratosphere. Stratospheric samples have a wider source footprint and are influenced by
265 troposphere-stratosphere exchange, and chemical reaction. In the stratosphere, the OH radical concentration on average decreases by a factor of 10 compared with tropospheric OH levels, whereas halogen radicals (e.g. chlorine (Cl) and bromine (Br)) are more abundant and react faster with ethane, methane and propane, therefore they play a greater relative role in ethane, methane and propane oxidation (Li et al., 2018). The loss of ethane in the stratosphere by reaction with Cl
270 radicals is about 40 times more than that by OH radicals (reaction rate of ethane with Cl is about 400 times faster than with OH at 250K (Atkinson et al., 2001), and stratospheric OH is about ten times more abundant than stratospheric Cl (Li et al., 2018)), whereas the ethane loss in the troposphere by Cl is negligible compared with by OH due to the small amounts of tropospheric Cl (OH:Cl around 10,000) (Lelieveld et al., 1999; Gromov et al., 2018)). The reaction rates of ethane,
275 methane and propane with Cl radicals are about 572:1:1330 at 298K (Atkinson et al., 1997), indicating that propane and ethane are more sensitive to the changes in stratospheric Cl radicals.

3.3.1 Linear trends in the lower stratosphere

Figure 5 shows the lower stratospheric observations, linear trends and moving average of ethane
280 (Figures 5 a,b,c,d,e), methane (Figures 5 f,g,h,i,j) and propane (Figures 5 k,l,m,n,o) over five regions: whole Northern Hemisphere (Figures 5 a,f,k), Europe (Figures 5 b,g,l), North America (Figures 5 c,h,m), Asia (Figures 5 d,i,n), and rest of the world (Figures 5 e,j,o). The growth rates of ethane, methane and propane over each region are shown in Table 2 b.

The growth rates of lower stratospheric methane over all five regions (range 0.22-0.51 %/yr) are
285 consistent with the upper tropospheric methane (range 0.29-0.37 %/yr) (Table 2). In contrast, the

10

difference between the lower stratospheric and upper tropospheric propane growth rates is large (usually > 1.5%/yr), because propane has a higher sensitivity to stratospheric chlorine and shorter lifetime compared to methane. The lower stratospheric ethane has similar growth rates in the whole NH, EUR and RNH compared with the upper troposphere, whereas the difference occurs

290   in NAM and ASI. The Asian summer monsoon may be a reason to explain the different growth rates in ASI, although further investigation on the change in troposphere-stratosphere mixing and stratospheric chlorine in NAM is needed.

3.3.2 Non-linear trends in the lower stratosphere

295   The observed lower stratospheric ethane over the whole NH shows two exceptional peaks in 2010 and 2013 (Figure 6 a). The peak in 2010 is not seen at regional levels (NAM, ASI, EUR), which suggests global upward transport of the upper tropospheric ethane (peaking in 2010-2011) into the stratosphere and the important contribution from RNH. The second peak in 2013 can be due to the regional emission transport from the troposphere into the lowermost stratosphere as

300   such a peak is observed simultaneously over NAM, ASI and RNH, or due to changes in stratospheric sinks (e.g. OH or Cl radical concentration) as such peaks are seen for all three compounds.

Methane trends in the lower stratosphere show large variability during 2010-2014 over the whole NH, ASI and RNH, similar variability is present in the upper tropospheric methane trends (Figure

305   3), indicating a fluctuated upwards transport of surface emissions into the upper troposphere and stratosphere.

3.3.3 Monthly variation in the lower stratosphere

The lower stratospheric ethane mole fractions do not show strong seasonality, except that NAM

310   has a seasonal trend with one month later shift compared to the upper tropospheric NAM trend. The lower stratospheric ASI ethane shows the same timing peak in June with upper tropospheric ASI ethane which potentially indicates the intrusion of tropospheric air masses into the stratosphere due to Asian summer monsoon (Xiong et al., 2009; Park et al., 2007). There is little seasonality evident in the ethane mole fractions in the stratosphere. Since stratospheric aircraft measurement

315   campaigns are generally of short duration (several weeks), a direct comparison to previous data is

11

not possible, however, vertical column data obtained by ground based FTIR for 8-21km reported by Helmig et al. (2016) also showed no clear seasonal variation.

The lower stratospheric methane is observed to reach the lowest in March-May over all five regions. Propane in the lower stratosphere reaches the highest in June-August over most regions
320   except ASI.

3.3.4 Trends in the lower and upper parts of the lower stratosphere

Because the potential vorticity of the lower stratospheric samples has a broad range (2-12.2 PVU), the lower stratosphere is further classified into two parts: lower part ($2 \leq PV < 6$ PVU) and
325   upper part ($PV \geq 6$ PVU), to investigate the changes of trends within the lower stratosphere. It is noted that the sample number of each sub-region gets smaller (95-1,656 samples per region; Table 2) by applying this classification, thus the trends have larger uncertainties and should be interpreted with caution.

The linear trends of methane over all five regions, and ethane over four regions (except ASI)
330   show little difference between the lower and upper parts of the lower stratosphere (Table 2 c,d; Figures S4-5). Larger differences (delta > 2%) in growth rates of ethane in ASI, and propane over all five regions are found.

The non-linear trends of ethane, methane and propane in the upper and lower parts of the lower stratosphere are similar over most regions (Figures S6-7). A significant difference occurs for
335   ethane in ASI during 2006-2013 when the lower part ethane had a sharp increase in 2006-2007, then followed a plateau in 2007-2013, whereas the upper part ethane had a continuous decrease in 2006-2013. It's noted that the sample number in upper part of the lower stratosphere over ASI is the minimum among all the sub-regions (Table 2).

340   ## 3.4 Limitations and implications

Despite the usefulness, uniqueness and high quality of our datasets, several limitations of our study should be noted. (a) Representativeness of the presented trends. Although our flight sampling is frequent and covers a large area of the NH, the spatial and temporal distributions of our samples

are not even. This may cause the trends being influenced by specific regions where more samples

345   were collected. (b) Nature of samples. Our samples were collected in the UTLS region and can be influenced by atmospheric transport (e.g. troposphere-stratosphere exchange), surface sources, and chemical destruction processes. Therefore, the trends represent the net effects of these factors making the interpretation with regard to single factors difficult. It is noted that our aircraft samples have significantly different spatial distributions compared with the studies summarized in the

350   Introduction section, therefore, any comparison should be carefully made. When comparing surface and airborne datasets from multiple locations to assess global atmospheric changes, it will become increasingly important to ensure comparability of data quality. A process that has begun through the grounding of a World Calibration Center for VOCs, although this dataset predates this initiative. (c) PV choice of identifying upper tropospheric and stratospheric samples. In this study,

355   we used PV=2 to define the tropopause, whereas other approaches exist. It is shown that on large space and time scales in the extratropics, the WMO thermal tropopause corresponds to a surface of constant potential vorticity (PV), although there exist systematic differences on smaller scales (Stohl et al., 2003; Wirth, 2000).

Implications. (a) Observations of ethane, methane and propane were often restricted at regional

360   scale or short-duration. We have presented a long-term (10 years) airborne observations of ethane, methane and propane in the UTLS region at northern hemispheric scale. This dataset is unique and can be used to examine long-term troposphere-stratosphere exchange, chemical and dynamical changes in the UTLS region, and improve model performance. To the best of our knowledge, such long-term aircraft observations are only available from IAGOS-CARIBIC

365   project (our study) and CONTRAIL project (Machida et al., 2008; Sawa et al., 2015). (b) The "Prophet" algorithm is an open source software, and suitable for non-continuous time-series datasets. Unlike the commonly used linear fit approach for trend analysis, the "Prophet" algorithm is robust to missing data and the influence from outliers is minimized. It better captures the inter-annual variability and is not influenced by the time period of choice. (c) Other analysis

370   approaches such as machine learning techniques can be used on our dataset to enlarge the spatial and temporal distributions. Combining our dataset with space-borne observations will provide a better view of global distributions and trends of trace gases.

4 Data availability

375   The IAGOS-CARIBIC observational data of ethane, methane, and propane in the period February 2006 – February 2016 can be accessed at https://doi.org/10.5281/zenodo.6536109 (Li et al., 2022). Co-authorship may be appropriate if the IAGOS-CARIBIC data are essential for a result or conclusion of a publication.

380   ## 5 Conclusions

In this study, we present upper tropospheric and lower stratospheric ethane trends from airborne observations over the period 2006-2016 with reference to methane and propane. The linear trends, moving averages, non-linear trends and monthly variations of ethane, methane and propane were examined for 20 sub-regions (4 categories: the upper troposphere, the lower

385   stratosphere, the lower part of the lower stratosphere, and the upper part of the lower stratosphere; and 5 regions under each category: whole NH, EUR, NAM, ASI and RNH). The linear trends of methane were similar in all sub-regions (range 0.22-0.51 %/yr increase), whereas ethane and propane had more variable trends due to their shorter atmospheric lifetime. The observed annual rates of change in atmospheric abundances of ethane, methane, and propane over

390   2006-2016 in the upper troposphere are -2.24, 0.33, and -0.78 %/yr, respectively, and in the lower stratosphere are -3.27, 0.26, and -4.91 %/yr, respectively. The dataset is publicly available and is valuable for future studies to evaluate and improve atmospheric models and emission inventories, and understand long-term changes in troposphere-stratosphere exchange and in sources and sinks of ethane, methane and propane.

395

Author contribution

M.L. and J.W. developed the idea of this study. M.L. wrote the first draft of the manuscript. All authors contributed to discussing and revising the manuscript.

400

Competing interests

The authors declare no conflict of interests.

410 **References**

Angelbratt, J., Mellqvist, J., Simpson, D., Jonson, J. E., Blumenstock, T., Borsdorff, T., Duchatelet, P., Forster, F., Hase, F., Mahieu, E., De Mazière, M., Notholt, J., Petersen, A. K., Raffalski, U., Servais, C., Sussmann, R., Warneke, T., and Vigouroux, C.: Carbon monoxide (CO) and ethane (C2H6) trends from ground-based solar FTIR measurements at six European 415 stations, comparison and sensitivity analysis with the EMEP model, Atmos. Chem. Phys., 11, 9253-9269, 10.5194/acp-11-9253-2011, 2011.

Angot, H., Davel, C., Wiedinmyer, C., Pétron, G., Chopra, J., Hueber, J., Blanchard, B., Bourgeois, I., Vimont, I., Montzka, S. A., Miller, B. R., Elkins, J. W., and Helmig, D.: Temporary pause in the growth of atmospheric ethane and propane in 2015–2018, Atmos. Chem. 420 Phys. , 2021, 1-34, 10.5194/acp-2021-285, 2021.

Atkinson, R., Baulch, D., Cox, R., Hampson Jr, R., Kerr, J., Rossi, M., and Troe, J.: Evaluated kinetic, photochemical and heterogeneous data for atmospheric chemistry: Supplement V. IUPAC Subcommittee on Gas Kinetic Data Evaluation for Atmospheric Chemistry, Journal of Physical and Chemical Reference Data, 26, 521-1011, 1997.

425 Atkinson, R., Baulch, D., Cox, R., Crowley, J., Hampson Jr, R., Kerr, J., Rossi, M., and Troe, J.: Summary of evaluated kinetic and photochemical data for atmospheric chemistry, IUPAC Subcommittee on gas kinetic data evaluation for atmospheric chemistry, 20, 2001.

Baker, A. K., Slemr, F., and Brenninkmeijer, C. A. M.: Analysis of non-methane hydrocarbons in air samples collected aboard the CARIBIC passenger aircraft, Atmos. Meas. Tech., 3, 311-321, 430 10.5194/amt-3-311-2010, 2010.

Baker, A. K., Schuck, T. J., Brenninkmeijer, C. A., Rauthe-Schöch, A., Slemr, F., van Velthoven, P. F., and Lelieveld, J.: Estimating the contribution of monsoon-related biogenic production to

methane emissions from South Asia using CARIBIC observations, Geophysical research letters, 39, 2012.

435 Brenninkmeijer, C. A. M., Crutzen, P., Boumard, F., Dauer, T., Dix, B., Ebinghaus, R., Filippi, D., Fischer, H., Franke, H., Frieβ, U., Heintzenberg, J., Helleis, F., Hermann, M., Kock, H. H., Koeppel, C., Lelieveld, J., Leuenberger, M., Martinsson, B. G., Miemczyk, S., Moret, H. P., Nguyen, H. N., Nyfeler, P., Oram, D., O'Sullivan, D., Penkett, S., Platt, U., Pupek, M., Ramonet, M., Randa, B., Reichelt, M., Rhee, T. S., Rohwer, J., Rosenfeld, K., Scharffe, D., Schlager, H.,

440 Schumann, U., Slemr, F., Sprung, D., Stock, P., Thaler, R., Valentino, F., van Velthoven, P., Waibel, A., Wandel, A., Waschitschek, K., Wiedensohler, A., Xueref-Remy, I., Zahn, A., Zech, U., and Ziereis, H.: Civil Aircraft for the regular investigation of the atmosphere based on an instrumented container: The new CARIBIC system, Atmos. Chem. Phys., 7, 4953-4976, 10.5194/acp-7-4953-2007, 2007.

445 Dalsøren, S. B., Myhre, G., Hodnebrog, Ø., Myhre, C. L., Stohl, A., Pisso, I., Schwietzke, S., Höglund-Isaksson, L., Helmig, D., Reimann, S., Sauvage, S., Schmidbauer, N., Read, K. A., Carpenter, L. J., Lewis, A. C., Punjabi, S., and Wallasch, M.: Discrepancy between simulated and observed ethane and propanelevels explained by underestimated fossil emissions, Nature Geoscience, 11, 178-184, 10.1038/s41561-018-0073-0, 2018.

450 Fischer, E. V., Jacob, D. J., Yantosca, R. M., Sulprizio, M. P., Millet, D. B., Mao, J., Paulot, F., Singh, H. B., Roiger, A., Ries, L., Talbot, R. W., Dzepina, K., and Pandey Deolal, S.: Atmospheric peroxyacetyl nitrate (PAN): a global budget and source attribution, Atmos. Chem. Phys., 14, 2679-2698, 10.5194/acp-14-2679-2014, 2014.

Franco, B., Bader, W., Toon, G. C., Bray, C., Perrin, A., Fischer, E. V., Sudo, K., Boone, C. D.,
455 Bovy, B., Lejeune, B., Servais, C., and Mahieu, E.: Retrieval of ethane from ground-based FTIR solar spectra using improved spectroscopy: Recent burden increase above Jungfraujoch, Journal of Quantitative Spectroscopy and Radiative Transfer, 160, 36-49, 10.1016/j.jqsrt.2015.03.017, 2015.

Franco, B., Mahieu, E., Emmons, L. K., Tzompa-Sosa, Z. A., Fischer, E. V., Sudo, K., Bovy, B.,
460 Conway, S., Griffin, D., Hannigan, J. W., Strong, K., and Walker, K. A.: Evaluating ethane and methane emissions associated with the development of oil and natural gas extraction in North America, Environmental Research Letters, 11, 044010, 10.1088/1748-9326/11/4/044010, 2016.

Gardiner, T., Forbes, A., de Mazière, M., Vigouroux, C., Mahieu, E., Demoulin, P., Velazco, V., Notholt, J., Blumenstock, T., Hase, F., Kramer, I., Sussmann, R., Stremme, W., Mellqvist, J.,
465 Strandberg, A., Ellingsen, K., and Gauss, M.: Trend analysis of greenhouse gases over Europe measured by a network of ground-based remote FTIR instruments, Atmos. Chem. Phys., 8, 6719-6727, 10.5194/acp-8-6719-2008, 2008.

González Abad, G., Allen, N. D. C., Bernath, P. F., Boone, C. D., McLeod, S. D., Manney, G. L., Toon, G. C., Carouge, C., Wang, Y., Wu, S., Barkley, M. P., Palmer, P. I., Xiao, Y., and Fu, T.
470 M.: Ethane, ethyne and carbon monoxide concentrations in the upper troposphere and lower stratosphere from ACE and GEOS-Chem: a comparison study, Atmospheric Chemistry and Physics, 11, 9927-9941, 10.5194/acp-11-9927-2011, 2011.

Gromov, S., Brenninkmeijer, C. A., and Jöckel, P.: A very limited role of tropospheric chlorine as a sink of the greenhouse gas methane, Atmospheric Chemistry and Physics, 18, 9831-9843,
475 2018.

Hausmann, P., Sussmann, R., and Smale, D.: Contribution of oil and natural gas production to renewed increase in atmospheric methane (2007–2014): top–down estimate from ethane and methane column observations, Atmos. Chem. Phys., 16, 3227-3244, 10.5194/acp-16-3227-2016, 2016.

480   Helmig, D., Rossabi, S., Hueber, J., Tans, P., Montzka, S. A., Masarie, K., Thoning, K., Plass-Duelmer, C., Claude, A., Carpenter, L. J., Lewis, A. C., Punjabi, S., Reimann, S., Vollmer, M. K., Steinbrecher, R., Hannigan, J. W., Emmons, L. K., Mahieu, E., Franco, B., Smale, D., and Pozzer, A.: Reversal of global atmospheric ethane and propane trends largely due to US oil and natural gas production, Nature Geoscience, 9, 490-495, 10.1038/ngeo2721, 2016.

485   Karu, E., Li, M., Ernle, L., Brenninkmeijer, C. A., Lelieveld, J., and Williams, J.: Atomic emission detector with gas chromatographic separation and cryogenic pre-concentration (CryoTrap-GC-AED) for trace gas measurement, Atmospheric Measurement Techniques, 10.5194/amt-2020-199, 2021.

Kort, E. A., Smith, M. L., Murray, L. T., Gvakharia, A., Brandt, A. R., Peischl, J., Ryerson, T. B.,
490   Sweeney, C., and Travis, K.: Fugitive emissions from the Bakken shale illustrate role of shale production in global ethane shift, Geophysical Research Letters, 43, 4617-4623, https://doi.org/10.1002/2016GL068703, 2016.

Lelieveld, J., Bregman, A., Scheeren, H., Ström, J., Carslaw, K., Fischer, H., Siegmund, P., and Arnold, F.: Chlorine activation and ozone destruction in the northern lowermost stratosphere,
495   Journal of Geophysical Research: Atmospheres, 104, 8201-8213, 1999.

Li, M., Pozzer, A., Lelieveld, J., and Williams, J.: Northern hemispheric atmospheric ethane trends (2006-2016) with reference to methane and propane [dataset], 10.5281/zenodo.6536109, 2021.

Li, M., Karu, E., Ciais, P., Lelieveld, J., and Williams, J.: The empirically determined integrated
500   atmospheric residence time of carbon dioxide (CO2), in review, 2022.

Li, M., Karu, E., Brenninkmeijer, C., Fischer, H., Lelieveld, J., and Williams, J.: Tropospheric OH and stratospheric OH and Cl concentrations determined from CH_4, CH_3Cl, and SF_6 measurements, Nature Climate and Atmospheric Science, 1, 10.1038/s41612-018-0041-9, 2018.

Machida, T., Matsueda, H., Sawa, Y., Nakagawa, Y., Hirotani, K., Kondo, N., Goto, K.,
505   Nakazawa, T., Ishikawa, K., and Ogawa, T.: Worldwide measurements of atmospheric CO 2 and other trace gas species using commercial airlines, Journal of Atmospheric and Oceanic Technology, 25, 1744-1754, 2008.

Monks, S. A., Wilson, C., Emmons, L. K., Hannigan, J. W., Helmig, D., Blake, N. J., and Blake, D. R.: Using an Inverse Model to Reconcile Differences in Simulated and Observed Global
510   Ethane Concentrations and Trends Between 2008 and 2014, Journal of Geophysical Research: Atmospheres, 123, 11,262-211,282, https://doi.org/10.1029/2017JD028112, 2018.

Park, M., Randel, W. J., Gettelman, A., Massie, S. T., and Jiang, J. H.: Transport above the Asian summer monsoon anticyclone inferred from Aura Microwave Limb Sounder tracers, Journal of Geophysical Research: Atmospheres, 112, 2007.

515   Pozzer, A., Schultz, M. G., and Helmig, D.: Impact of U.S. Oil and Natural Gas Emission Increases on Surface Ozone Is Most Pronounced in the Central United States, Environmental Science & Technology, 54, 12423-12433, 10.1021/acs.est.9b06983, 2020.

Rudolph, J.: The tropospheric distribution and budget of ethane, Journal of Geophysical Research: Atmospheres, 100, 11369-11381, 10.1029/95JD00693, 1995.

520   Sawa, Y., Machida, T., Matsueda, H., Niwa, Y., Tsuboi, K., Murayama, S., Morimoto, S., and Aoki, S.: Seasonal changes of CO2, CH4, N2O, and SF6 in the upper troposphere/lower stratosphere over the Eurasian continent observed by commercial airliner, Geophysical Research Letters, 42, 2001-2008, 2015.

Schuck, T. J., Brenninkmeijer, C. A. M., Slemr, F., Xueref-Remy, I., and Zahn, A.: Greenhouse
525   gas analysis of air samples collected onboard the CARIBIC passenger aircraft, Atmos. Meas. Tech., 2, 449-464, 10.5194/amt-2-449-2009, 2009.

Simpson, I. J., Sulbaek Andersen, M. P., Meinardi, S., Bruhwiler, L., Blake, N. J., Helmig, D., Rowland, F. S., and Blake, D. R.: Long-term decline of global atmospheric ethane concentrations and implications for methane, Nature, 488, 490-494, 10.1038/nature11342, 2012.

530   Stohl, A., Bonasoni, P., Cristofanelli, P., Collins, W., Feichter, J., Frank, A., Forster, C., Gerasopoulos, E., Gäggeler, H., and James, P.: Stratosphere-troposphere exchange: A review, and what we have learned from STACCATO, Journal of Geophysical Research: Atmospheres, 108, 2003.

Sun, Y., Yin, H., Liu, C., Mahieu, E., Notholt, J., Té, Y., Lu, X., Palm, M., Wang, W., Shan, C.,
535   Hu, Q., Qin, M., Tian, Y., and Zheng, B.: Reduction in C2H6 from 2015 to 2020 over Hefei, eastern China points to air quality improvement in China, Atmos. Chem. Phys., 2021, 1-29, 10.5194/acp-2021-13, 2021.

Taylor, S. J. and Letham, B.: Forecasting at scale, The American Statistician, 72, 37-45, 2018.

Tzompa-Sosa, Z. A., Mahieu, E., Franco, B., Keller, C. A., Turner, A. J., Helmig, D., Fried, A.,
540   Richter, D., Weibring, P., Walega, J., Yacovitch, T. I., Herndon, S. C., Blake, D. R., Hase, F., Hannigan, J. W., Conway, S., Strong, K., Schneider, M., and Fischer, E. V.: Revisiting global fossil fuel and biofuel emissions of ethane, Journal of Geophysical Research: Atmospheres, 122, 2493-2512, https://doi.org/10.1002/2016JD025767, 2017.

Wirth, V.: Thermal versus dynamical tropopause in upper-tropospheric balanced flow anomalies,
545   Quarterly Journal of the Royal Meteorological Society, 126, 299-317, 2000.

Xiong, X., Houweling, S., Wei, J., Maddy, E., Sun, F., and Barnet, C.: Methane plume over south Asia during the monsoon season: satellite observation and model simulation, Atmospheric Chemistry and Physics, 9, 783-794, 2009.

550

Figures and Tables

Table 1. Summary of studies reporting ethane trends in the (a) troposphere and (b) stratosphere.
555 Parentheses in first column indicates the locations of measurements.

Trends (%/year)	Time period	References
(a) Tropospheric trends		
-1.09 ~ -2.11	1996-2006	Angelbratt et al. (2011)
(four European sites)		
-0.81 (global)	1986-2010	Simpson et al. (2012)
-0.92 (Jungfraujoch, 47° N)	1994-2008	Franco et al. (2015)
4.9 (Jungfraujoch, 47° N)	2009-2014	Franco et al. (2015)
2.9-4.7 (32 ground sites)	2009-2014	Helmig et al. (2016)
3-5 (six sites)	2009-2014	Franco et al. (2016)
	compared with 2003-2008	
ca. 4.6 (Zugspitze, 47° N)	2007-2014	Hausmann et al. (2016)
ca. -2.5 (Lauder, 45° S)	2007-2014	Hausmann et al. (2016)
ca. 5.6 (GEOSummit, 73° N)	01.2010-12.2014	Angot et al. (2021)
-2.6 ± 1.34 (Hefei, 32° N)	2015-2020	Sun et al. (2021)
(b) Stratospheric trends		
-3.31 ~ 0.43	2000-2005	Gardiner et al. (2008)
(stratospheric column)		
-1.75 ± 1.30	2004-2008	Franco et al. (2015)
(8-16km above Jungfraujoch)		
-1.0 ± 0.2	1995-2009	Helmig et al. (2016)
(8-21km above Jungfraujoch)		
9.4 ± 3.2	2009-2013	Franco et al. (2015)
(8-16km above Jungfraujoch)		
6.0 ± 1.1	2009-2015	Helmig et al. (2016)
(8-21km above Jungfraujoch)		

560   Table 2. Sample number and linear trends of ethane, methane and propane.

	Sample number	Linear trend (2006-2016)					
		C_2H_6(ppt/yr)	C_2H_6(%/yr)*	CH_4(ppb/yr)	CH_4(%/yr)*	C_3H_8(ppt/yr)	C_3H_8(%/yr)*
(a)Upper troposphere (Altitude ≥8000m, PV<2)							
Whole NH	3288	-14.90	-2.24	5.80	0.33	-0.70	-0.78
EUR	364	-11.10	-1.33	6.70	0.37	3.20	2.07
NAM	1023	-17.10	-2.33	6.50	0.36	1.10	0.90
ASI	634	-6.90	-1.17	5.20	0.29	0.30	0.33
RNH	1267	-26.70	-5.19	5.90	0.33	-7.50	-14.73
(b)Lower stratosphere (PV≥2)							
Whole NH	3245	-17.60	-3.27	4.70	0.26	-3.60	-4.91
EUR	448	-8.70	-1.61	6.50	0.37	-4.60	-5.42
NAM	420	8.50	2.28	9.00	0.51	4.10	11.87
ASI	324	-19.20	-4.55	4.20	0.24	-4.40	-7.55
RNH	2053	-22.80	-4.33	4.00	0.22	-4.70	-6.70
(c)Lower stratosphere (lower part; 2≤PV<6)							
Whole NH	1589	-10.90	-1.69	6.70	0.38	-2.50	-2.42
EUR	226	-20.00	-2.89	6.00	0.33	-7.90	-7.20
NAM	154	-10.50	-1.95	8.90	0.50	7.00	15.05
ASI	229	-14.40	-3.25	5.50	0.31	-4.10	-7.11
RNH	980	-11.30	-2.04	6.70	0.38	-2.40	-3.24
(d)Lower stratosphere (upper part; PV≥6)							
Whole NH	1656	-8.40	-2.99	5.90	0.34	-2.90	-10.21
EUR	222	-9.00	-3.53	3.70	0.22	-2.10	-9.33
NAM	266	6.70	3.27	6.50	0.37	0.50	3.46
ASI	95	-17.50	-5.83	4.30	0.25	-3.60	-12.84
RNH	1073	-10.30	-4.01	6.80	0.39	-4.10	-24.84

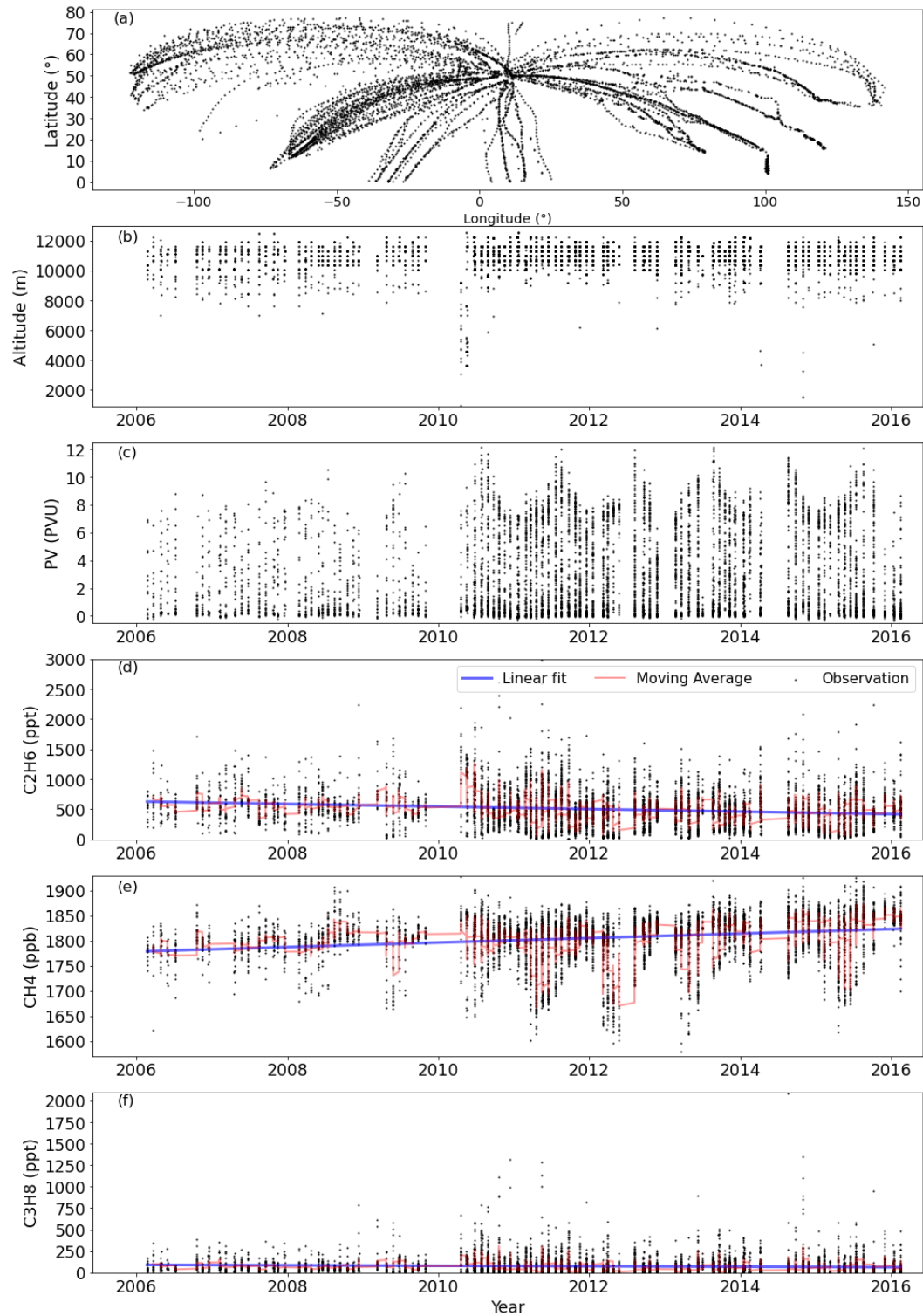*growth rate relative to rolling average of first 20 observations of the dataset of each region.

Figure 1. Data overview of (a) geographical distribution; (b) altitude; (c) potential vorticity (PV); mole fractions of (d) ethane; (e) methane; (f) propane.
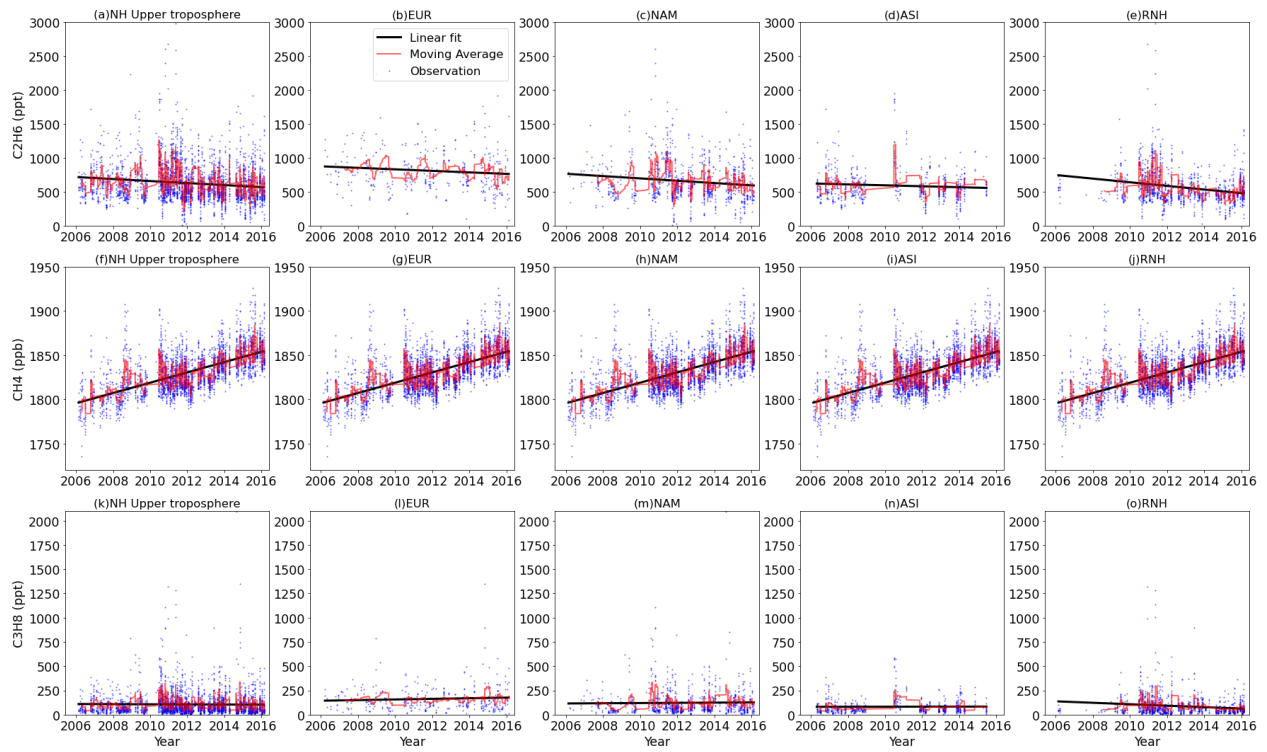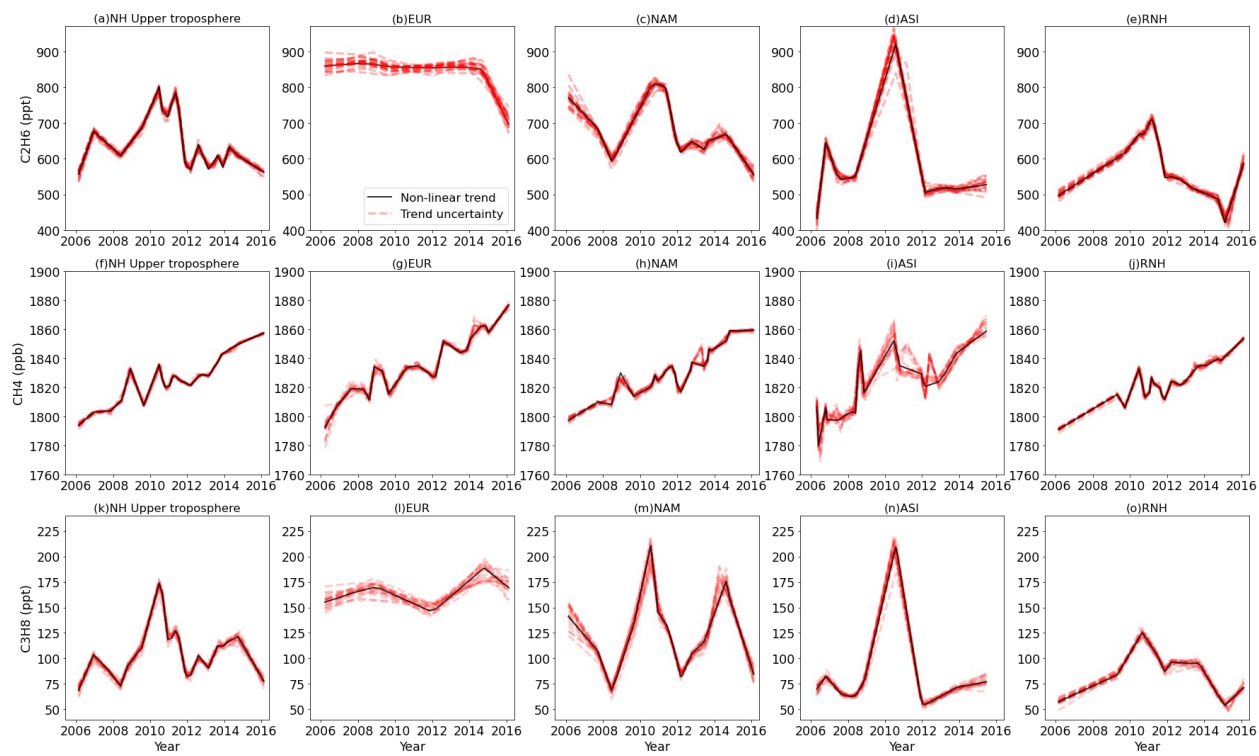
Figure 2. The upper tropospheric ethane, methane and propane mole fractions from observations
and linear trends over five regions (whole NH upper troposphere, EUR, NAM, ASI, and RNH).

575

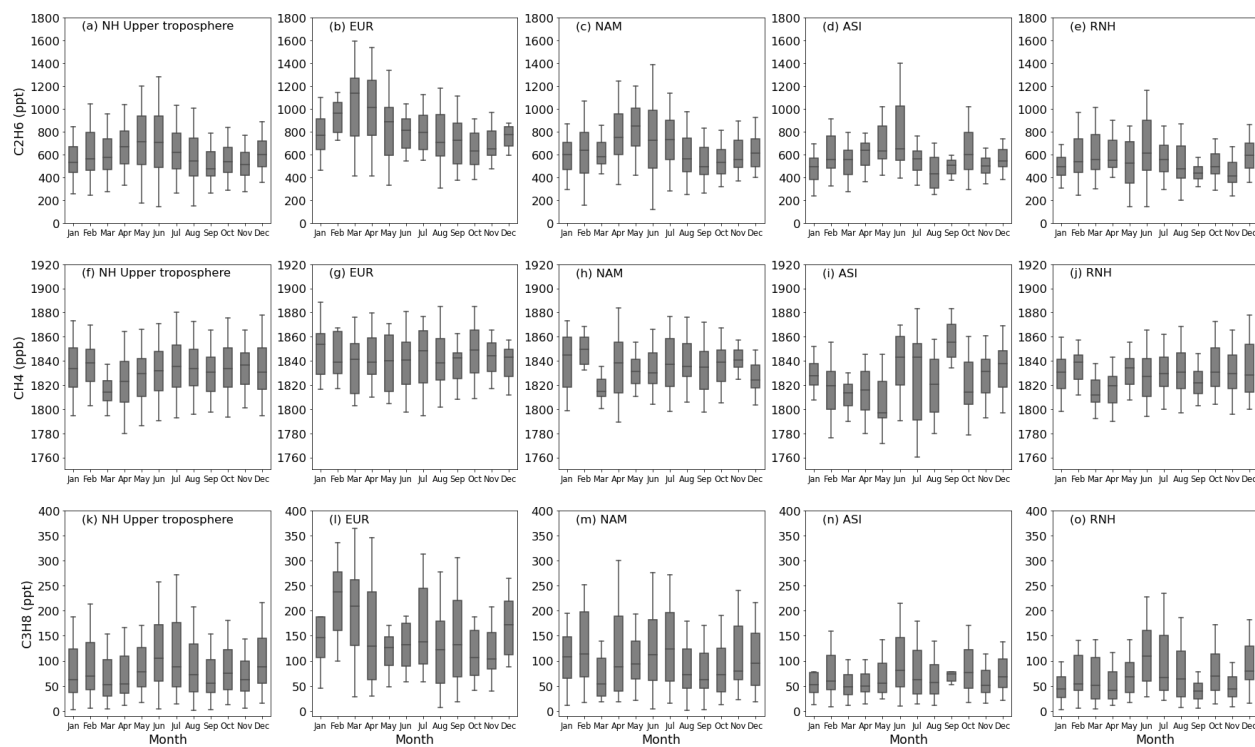Figure 3. Non-linear trends of the upper tropospheric ethane, methane and propane over five regions (whole NH upper troposphere, EUR, NAM, ASI, and RNH).
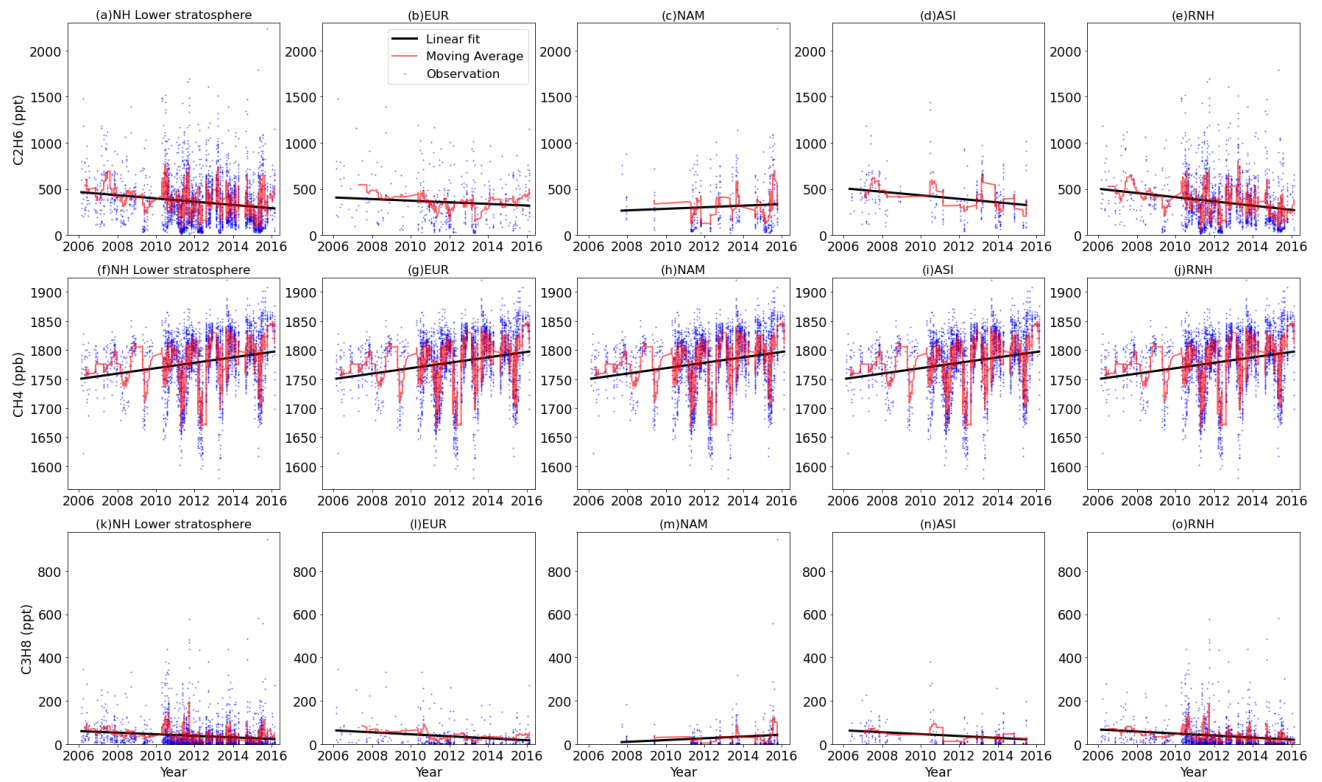
Figure 4. Monthly variations of the upper tropospheric ethane, methane and propane (2006-2016) over five regions (whole NH, EUR, NAM, ASI and RNH). The boxes represent 25%-75% of all observed mole fractions, the horizontal lines in the boxes indicate the medians. The whiskers represent the 10%-90% range of all the observed mole fractions.

590

Figure 5. Lower stratospheric ethane, methane and propane mole fractions from observations and linear trends over five regions (whole NH lower stratosphere, EUR, NAM, ASI, and RNH).
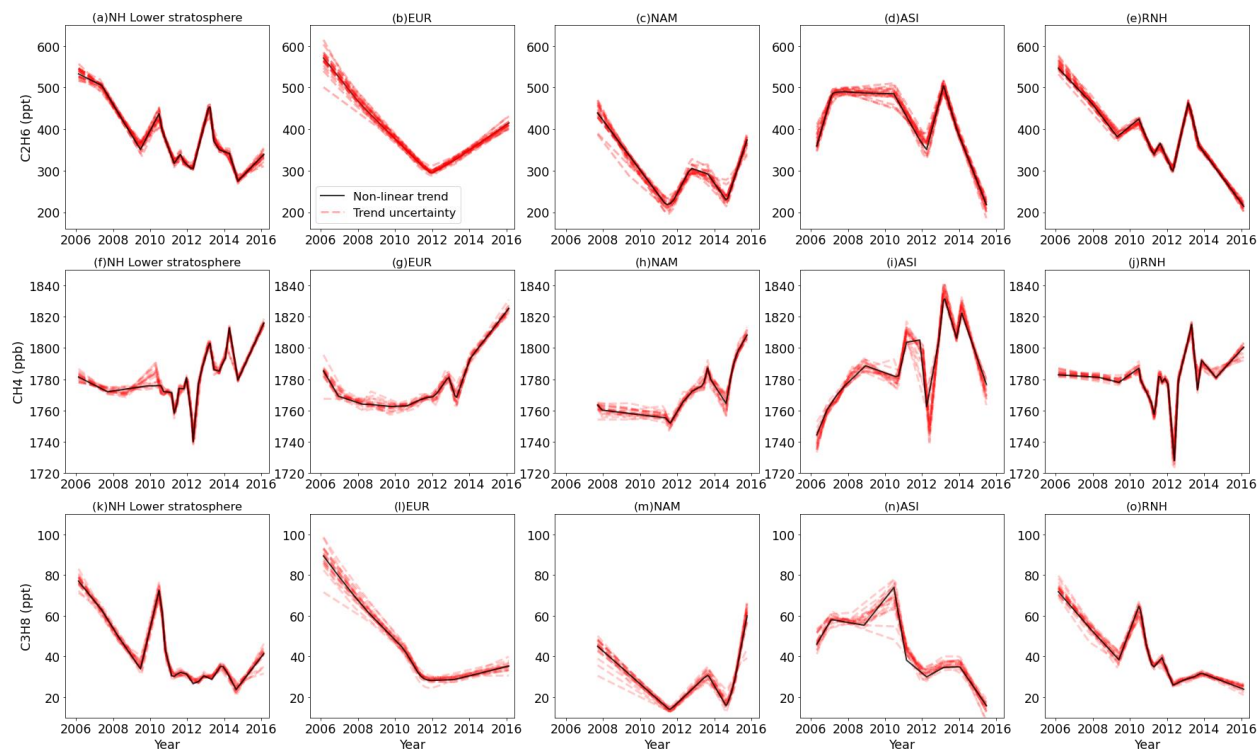
595

Figure 6. Non-linear trends of the lower stratospheric ethane, methane and propane over five regions (whole NH lower stratosphere, EUR, NAM, ASI, and RNH).
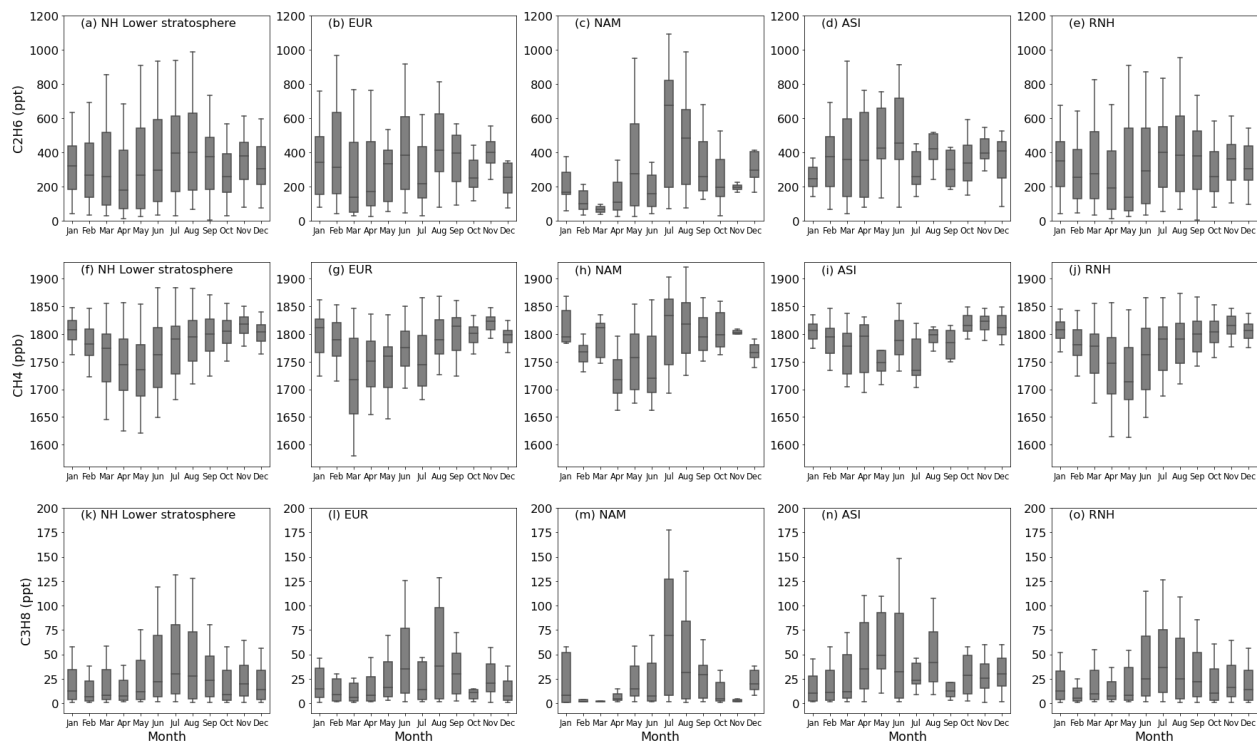
600

Figure 7. Monthly variations of the lower stratospheric ethane, methane and propane (2006-2016)
over five regions (whole NH, EUR, NAM, ASI and RNH). The boxes represent 25%-75% of all
observed mole fractions, the horizontal lines in the boxes indicate the medians. The whiskers
represent the 10%-90% range of all the observed mole fractions.